



Oil palm age estimation using broad-band and narrow-band vegetation indices derived from Sentinel-2 data

Angeli N. Jarayee¹, Helmi Z. M. Shafri^{1*}, Yuhao Ang¹, Yang P. Lee², Shahrul A. Bakar², Haryati Abidin², Hwee S. Lim³, Rosni Abdullah⁴, Umar U. M. Junaidi⁵, and Na'aim Samad²

¹Department of Civil Engineering and Geospatial Information Science Research Centre (GISRC), Faculty of Engineering, Universiti Putra Malaysia (UPM), Serdang, Selangor, Malaysia

²Geoinformatics Unit, FGV Sdn Bhd, FGV Innovation Centre, Lengkuk Teknologi, Bandar Enstek, Negeri Sembilan, Malaysia.

³School of Physics, Universiti Sains Malaysia (USM), Gelugor, Penang, Malaysia.

⁴School of Computer Sciences, Universiti Sains Malaysia (USM), Gelugor, Penang, Malaysia.

⁵FGV Agri Services Sdn Bhd, Level 9, West, Wisma FGV, Jalan Raja Laut, Kuala Lumpur, Malaysia.

*Corresponding author: helmi@upm.edu.my

Received 3 October 2022

Revised 1 February 2023

Accepted 16 February 2023

Abstract

In the past, the monitoring of crops in the agriculture sector was done manually. However, this approach is inconvenient as it consumes time, energy, and money. Various vegetation indices obtained through remote sensing data are utilized to monitor vegetation development. One main factor affecting the oil palm's production and health is its age. Therefore, this study aimed to determine the relationship between vegetation indices (VIs) and the age of oil palm using polynomial regression and to predict the oil palm age by generating the spatial distribution map. The data used were raw data that consisted of the oil palm age and its boundaries and the satellite data, Sentinel-2 imagery. There were four VIs used in this study: Normalized Difference Vegetation Index (NDVI), Normalized Difference Red Edge (NDRE), Chlorophyll Content Index (CCI), and Soil Adjusted Vegetation Index (SAVI). Among these VIs, CCI achieved the best overall accuracy with $R^2 = 0.94$, and the age of oil palm can be predicted using the equation $y = -4.6062x^2 + 27.864x + 14.169$. The findings demonstrate that the narrow-band vegetation index can effectively identify the spatial variation in the ages of oil palm trees and serve as an inventory for decision-making.

Keywords: Oil palm age, Remote sensing, Vegetation indices, Spatial distribution map

1. Introduction

The oil palm industry is a Malaysian agricultural sector that primarily contributes to Malaysia's economy by generating income from export activities and providing job opportunities. In 2020, this sector utilized approximately 5.2 million hectares of land in Malaysia for cultivation. Monitoring the development of plants in the agriculture sector was done manually in the olden days. However, this approach is no longer feasible considering the large-scale cultivation of oil palm trees. Monitoring oil palm trees' conditions on this scale requires a lot of money and human power. Thanks to technological advancement, remote sensing techniques have been used widely for various agriculture sector applications, such as detecting and calculating the number of trees and supervising vegetation healthiness. To effectively monitor the conditions of oil palm plantations and tree replanting, it is crucial to have accurate and detailed maps of the oil palm areas [1-4]. Satellite imagery such as Landsat-8 and Sentinel-2 is the data source for the oil palm plantation maps. Satellite images provide various data on the Earth's surface, usually obtained through aircraft or satellites. Studying through remote sensing is highly beneficial as it enables access to diverse locations, even those that are challenging to reach through transportation [5]. Therefore, remote sensing is widely adopted because of its ease of use, cost-effectiveness, and temporal

efficiency. Researchers can perform analysis virtually and obtain data in less time than conventional field-based methods.

In the agriculture industry, vegetation classification and monitoring are usually performed depending on the bands reflected by the leaf [6]. Furthermore, it is essential to determine the biophysical characteristics and properties of the oil palm to monitor its health. The vegetation indices (VIs) perform several other functions, such as determining the density and growth development of plants, chlorophyll contents, nutrients, biomass, yields, and other biophysical characteristics [7]. One of the most widely used VIs is the NDVI. Nonetheless, broad-band vegetation indices like NDVI tend to become saturated when crops are grown under a large canopy [8]. The problem can therefore be addressed by narrow-band vegetation indices, such as the NDRE and CCI, by including red edge bands that show rapid changes in reflectance, which directly associate with the biophysical properties of crops [9].

Identifying the age of the palm tree is significant since oil palm yield is closely associated with its growth throughout its lifespan. The optimal yield period for a palm tree is between nine to eighteen years of age, following which the yield capacity gradually decreases over time [10]. Past research studies have proven that remote sensing technology has the potential to estimate and map the age of oil palm in plantations [11-13]. [13] used Landsat-8 satellite image to generate four indices (advanced vegetation index, bare soil index, shadow index, and thermal index) and integrate them into the forest density canopy model for estimating oil palm age. [12] used NDVI from Landsat 8 satellite images to develop a regression model for estimating the age of oil palms and determining the distribution of oil palm age. Although the application of NDVI for age estimation has been reported in the literature, the studies of other types of VIs are still limited. Therefore, narrow-band vegetation indices should be utilized to estimate the age of oil palms, particularly for older palms with larger canopies.

The VIs used in this study include the NDVI, Soil Adjusted Vegetation Index (SAVI), Normalized Difference Red Edge (NDRE), and Chlorophyll Content Index (CCI). The main objective of this study was to predict the oil palm tree's age based on vegetation indices using Sentinel-2 image. This study will then generate the distribution map of the oil palm age based on the developed model inputted from vegetation indices.

2. Materials and methods

2.1 Study area

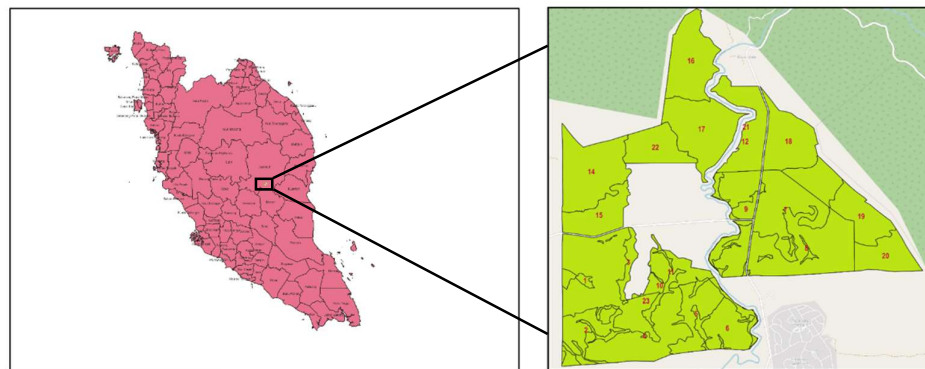


Figure 1 The study area.

The study area was in the North-Eastern Pahang in the Jerantut district, as shown in Figure 1. The plantation area consists of 23 blocks that cover approximately 24 km². This study area was chosen due to its variations in the oil palm age. The age range of oil palms in this study was between 5 and 28 years (Table 1). The data indicated a monthly increase in yields, suggesting that the palm trees in this area could be a suitable candidate for studying the effect of vegetation indices on their age.

Table 1 General information on a basic description of age across the blocks.

Information	Values
Ages	5-28 years old
Count	24
Mean	20
Standard deviation	7.16
Max	28
Min	5

2.2 Flowchart

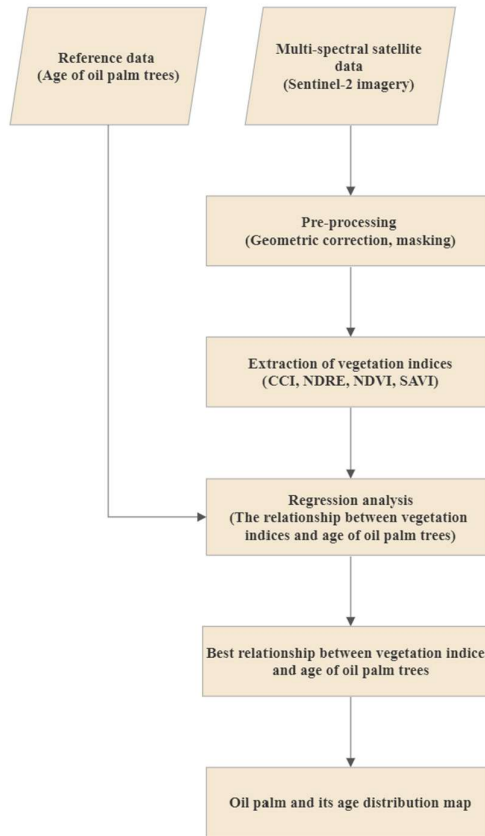


Figure 2 The flowchart of the study.

Figure 2 shows the methodology proposed to obtain the results discussed in Part 3 of this journal. It consists of several steps, including data acquisition using Quantum Geographic Information System (QGIS) and reference data received from Felda Global Ventures (FGV) Holdings Berhad. Satellite data, namely the Sentinel-2 image for the year 2020 obtained from QGIS, was pre-processed, and VIs were extracted from it. These VIs were used to conduct regression analysis to determine the relationship between VIs and the age of the oil palm tree. The final step was to generate the oil palm age distribution map based on the results from regression analysis.

2.3 Data acquisition

Two data used in this study were the reference and satellite imagery. The reference data used in this study consisted of the oil palm age and the plantation boundaries obtained from Felda Global Ventures (FGV) Holdings Berhad. Meanwhile, the satellite data was acquired from Sentinel-2 (S2) in QGIS 3.22 for the year 2020 using Semi-Classification Plugins (SCP). This data was used to generate vegetation indices in mapping the age distribution of oil palms. The primary purpose of S2 satellites being launched by the European Space Agency (ESA) under the Copernicus Programme was to improve and provide a higher spatial resolution of satellite information for the classification of land cover and land use (LULC), as well as to monitor the changes of climate and disaster. Additionally, it is well-suited for land cover monitoring, particularly in vegetation-rich areas such as agricultural plantations, forests, urban development areas, and wetlands. It has received positive feedback regarding its effectiveness [14].

S2 image is known as a multispectral satellite, consisting of 13 spectral bands (from near-infrared to shortwave infrared) and 10, 20, or 60 meters of spatial resolution for respective bands. This band combination from the satellite image has been used to obtain various data. This research used these band combinations to estimate the chlorophyll content in the oil palm tree leaves by ratio. For instance, the band combination of B4 (red), B3 (green), and B2 (blue), S2 images will generate a natural color which means it will produce an image just like how we see

it in reality. The S2 image had a 10% cloud cover percentage to create a cloud-free composite. Next, the S2 image was pre-processed by using a cloud masking method. The bands used in this research are shown in Table 2. The spatial resolutions of all satellite bands were resampled to 10 meters using the nearest neighbor method.

Table 2 The 13 bands in S2.

Band	Resolution (m)	Central Wavelength (nm)	Description
B1	60	443	Ultra-Blue (Coastal and Aerosol)
B2	10	490	Blue
B3	10	560	Green
B4	10	665	Red
B5	20	705	Visible and Near Infrared (VNIR)
B6	20	740	VNIR
B7	20	783	VNIR
B8	10	842	VNIR
B8a	20	865	VNIR
B9	60	940	Short Wave Infrared (SWIR) - Water Vapor
B10	60	1375	SWIR - Cirrus
B11	20	1610	SWIR
B12	20	2190	SWIR

2.4 Analysis of data

This study analyzed the data by rationing the bands in QGIS 3.22 and extracting the VIs from the generated maps. The values extracted from vegetation maps were used to create the regression modeling. The best relationship models closest to 1 were selected to develop the age spatial distribution map.

2.4.1 Spectral transformation

The VI is an essential quantified element that is important in the agriculture sector to monitor the healthiness and development of a plant. The value was calculated based on the bands of the satellite imagery acquired from remote sensing platforms, such as satellites, aircraft, and UAVs [15]. In this paper, four VIs were calculated based on the S2 image. These VI included NDVI, SAVI, NDRE, and CCI. Table 3 shows the formula used for the VI calculations in QGIS.

Table 3 The vegetation indices and formulas.

No.	Vegetation Index	Calculation	Reference
1.	NDVI	(NIR-R)/(NIR+R)	[16]
2.	NDRE	(NIR-RE)/(NIR+RE)	[17]
3.	SAVI	[(1+L)(NIR-R)]/(NIR+R+L)	[18]
4.	CCI	(NIR/RE)-1	[19]

2.4.1.1 Normalized Difference Vegetation Index (NDVI)

NDVI is the ratio of the difference in the near-infrared (NIR) and the red reflectance (R) to their total. The ratio is typically between -1 to 1, indicating the rate of photosynthesis in the plant. Healthy plants with high chlorophyll content, essential for photosynthesis, typically reflect at high NIR, resulting in a high NDVI [16]. Thus, it can be inferred that higher NDVI values indicate better plant health, whereas lower NDVI values suggest the presence of little or no vegetation.

2.4.1.2 Normalized Difference Red Edge (NDRE)

NDRE is the difference between the NIR and red edge (RE) bands divided by the sum of the NIR and RE bands. NDRE is usually used in the later phase of agriculture. Similar to NDVI, a higher NDRE value indicates plants with high levels of chlorophyll content and a healthy state. Compared to NDVI, NDRE can estimate the chlorophyll content in the tree canopy more accurately due to the RE bands [17].

2.4.1.3 Soil Adjusted Vegetation Index (SAVI)

SAVI is one of the vegetation indices used to reduce the brightness of the soil by using the correction factor (L) [18]. It is the ratio of the difference in NIR and red bands to the sum of NIR and red bands with a correction factor (L). The correction factor (L) value is often defined as 0.5, which reduces the influence of soil brightness when the vegetation area is sparsely distributed.

2.4.1.4 Chlorophyll Content Index (CCI)

CCI is the difference between the ratio of NIR to RE spectral bands and 1. The chlorophyll content in the leaves provides the necessary information about the health condition of the plants as measured by the rate of photosynthesis. The high chlorophyll content and photosynthesis rate indicate a healthy plant [19].

2.4.2 Regression modeling

Regression analysis can help determine the impact of one variable on another variable. In this study, we investigated how the age of the oil palm affects the vegetation indices (NDVI, NDRE, SAVI, and CCI). Due to the non-linear nature of the oil palm data in this study, polynomial regression models were utilized. To find the better fitting, we used the mean square error of polynomial regression to determine the suitable degree of polynomial [20]. The lower the mean square error, the better the model fits the data. We found that the best degree of polynomial fitting for the model was 2. The equation obtained was proven useful for estimating the age of oil palm trees, with the value of R^2 indicating the fitness of the model to the actual data. The nearer the value to 1, the better the model fits the data [21].

2.4.3 Oil palm age distribution mapping

This study generated the oil palm age distribution map in QGIS 3.22 using an interpolation method known as inverse distance weighting (IDW). A weighted average of the values recorded at the control point determined the weights allocated to the unsampled locations.

3. Results and Discussion

3.1 Relationship between vegetation indices and oil palm age

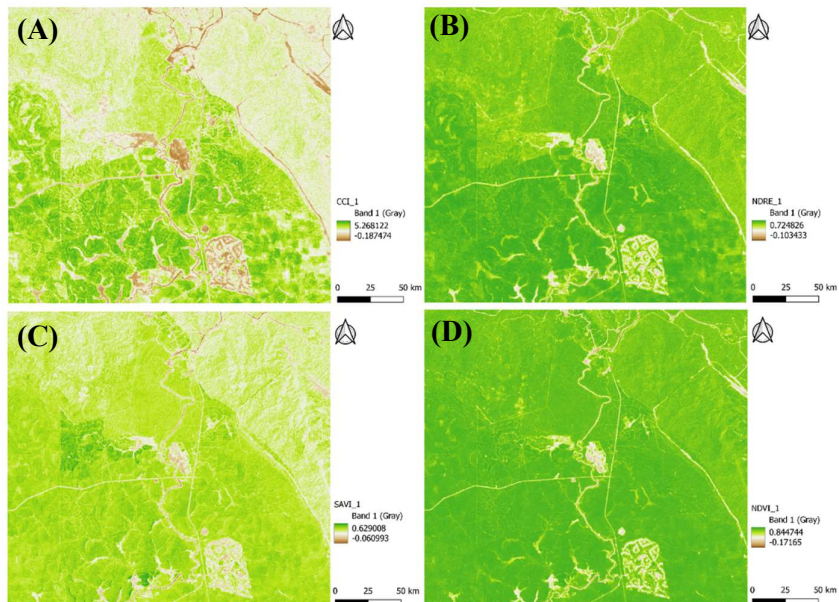


Figure 3 Vegetation indices maps: (A) CCI, (B) NDRE, (C) SAVI, and (D) NDVI.

VI's combines surface reflectance at two or more wavelengths to emphasize a specific vegetation characteristic based on reflectance. Each VI emphasizes a specific characteristic of the vegetation. Formulas in Table 2 were computed using the raster calculator, and the resulting vegetation indices (VI's) were reclassified to generate maps, as shown in Figure 3.

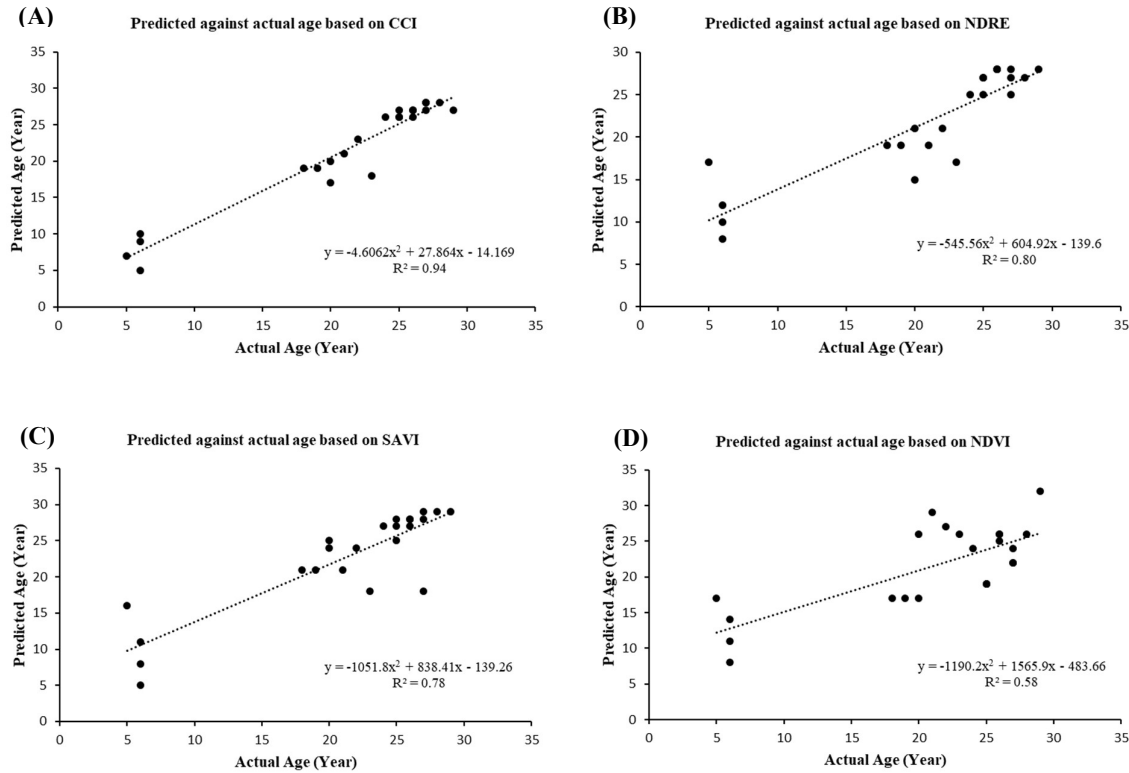


Figure 4 Scatter plots of the predicted age versus actual age of oil palm trees for polynomial regression in the year 2020. (A) CCI, (B) NDRE, (C) SAVI, and (D) NDVI.

Figure 4 depicts the relationship between the predicted and actual age of oil palm trees, as determined by polynomial regression. The graph for predicted age versus actual age using CCI yielded the highest R^2 value of 0.94.

The VI's were extracted from the respective VI's map of the study area, which consisted of 23 blocks. The extraction involved a random selection of the respective boundary and age. The extracted VI's were used to generate a regression model shown in Figure 5. The regression models were developed using the oil palm age data from FGV, and VI's extracted from S2 2020, as shown in Figure 5(A)–(D). The relationship between each VI and the oil palm age was visualized in a scatterplot. A scatterplot is a graph frequently used to observe the relationship between two variables. The data were fitted using polynomial regression with a degree order of two. The polynomial regression was chosen due to its flexibility in predicting the non-linear relationship between VI's and oil palm age. The coefficient of determination (R^2) values were obtained from these models, and the highest R^2 amongst these VI's was selected to generate the age distribution map. The range of R^2 is between 0 to 1. The closer the value of R^2 to 1, the lesser the discrepancies between the measured data and the predicted values.

Figure 5(A)–(D) shows the graphs representing the relationship between the oil palm age and the VI's. Figure 5 shows the results of the model and coefficient of determination (R^2) for CCI. CCI achieved the best overall accuracy among VI's with an $R^2 = 0.94$, indicating that 94% of the data variability fit the regression model. The equation, $y = -4.6062x^2 + 27.864x + 14.169$, was used to predict the age of oil palm. The CCI extracted from the S2 image demonstrated a good correlation with the oil palm age. The lowest R^2 showing the correlation between the oil palm age and NDVI was 0.58. During the growing stage, the value of NDVI is usually lower than SAVI ($R^2 = 0.78$) since SAVI uses soil-adjustment factors (L) for its analysis. SAVI can be another alternative adjusted index for NDVI because it can eliminate the noise of the soil background. Further explanation was provided by [22], who demonstrated that the negative soil adjustment factor was also a factor of the slope of vegetation contour and the

positive intersection points between vegetation isolines and soil. NDRE achieved better accuracy ($R^2= 0.80$) than NDVI and OSAVI because it comprises a red edge band that can penetrate deeper into the canopy of the plant's leaves. Additionally, CCI achieved the highest accuracy with an R^2 of 0.94 among other VIs. The results were consistent with most precision agriculture methods reported in previous studies [23][24]. A narrow vegetation index, such as NDRE and CCI, is highly responsive to changes in leaf reflectance, which coincide with the transition between chlorophyll absorption at the red wavelength and canopy scattering at the NIR wavelength [25][26]. Our results demonstrate that the narrow band vegetation index is the best indicator for estimating oil palm age, which surpasses the previous work of [12] that used NDVI to estimate oil palm age.

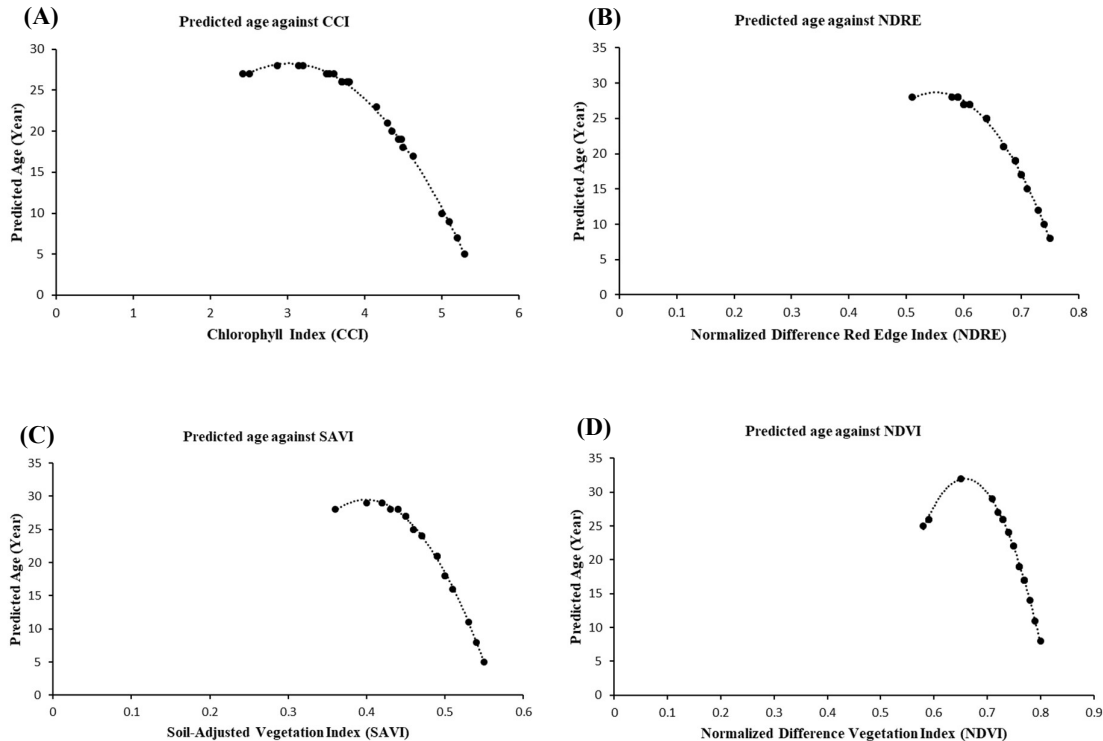


Figure 5 The trend in the age of oil palm trees against VIs: (A) CCI, (B) NDRE, (C) SAVI, and (D) NDVI.

Figure 5 (A)–(D) exhibits a consistent pattern across all graphs, with a decrease in vegetation indices (VIs) observed as oil palm trees age. Oil palm trees typically have a lifespan of 25 to 30 years before they are replaced by replanting. The young oil palm trees showed lower VIs. At their prime age (10 to 24 years), the VIs increased significantly, and in mature age (>25 years), the value decreased. As the plant ages, the rate of photosynthesis decreases, and the amount of chlorophyll degrades, resulting in a low VI. Crop yields are typically highest between 9 to 18 years, after which they decline. High yields also indicate the high usage of chlorophyll for photosynthesis, as exhibited in increased VIs.

3.2 Oil palm mapping

A spatial distribution map was used to show the density of the oil palm in the study area based on their age. The map was generated by calculating the predicted oil palm age based on the model equation obtained through regression analysis.

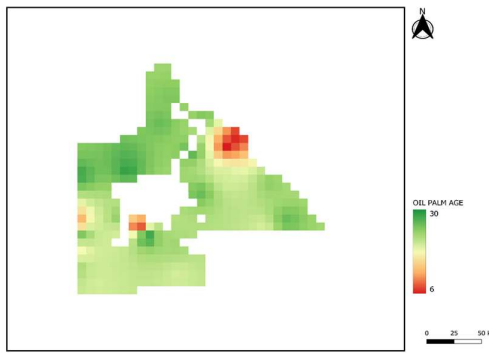


Figure 6 Spatial age distribution map.

Generated using spatial interpolation called inverse distance weighting (IDW), the spatial age distribution map shows the density of the oil palm trees according to their age. In Figure 6, younger oil palm trees are depicted as red, while the progressively darker shades of green correspond to older trees. The results demonstrate that most oil palm trees in the study area were mature (age > 20 years). With the information extracted from the spatial maps, management can accurately plan replanting programs to maintain oil palm yield production.

4. Conclusion

The findings demonstrate the effective use of narrow and broad-band vegetation indices for developing the model to estimate oil palm age. The result shows that the narrow-band vegetation index is the best indicator for estimating the oil palm age compared to broad-band vegetation indices. There is a moderate correlation between CCI and oil palm age. As the age of oil palm increases, the value of vegetation indices (VIs) decreases. Compared to other VIs, CCI achieved the best overall accuracy with an $R^2 = 0.94$, and the age of the oil palm was predicted using $y = -4.6062x^2 + 27.864x + 14.169$. Based on the spatial distribution maps, the density of the oil palm trees based on their age was determined. Future studies should focus on assessing the distribution of oil palm age within blocks to ascertain the actual coverage areas based on age. Efforts should be made to validate the relationship between chlorophyll content and oil palm age using SPAD readings. The findings will aid in developing a comprehensive mapping procedure for the plantation. Developing comprehensive mapping procedures for the palm age can help establish an inventory for the oil palm age and may be effective for the ground census operation so that any loss of information can be avoided.

5. Acknowledgements

The authors would like to acknowledge the Ministry of Higher Education (MOHE), Malaysia for providing the necessary resources and financial support through the Long-Term Research Grant Scheme (LRGS)-Malaysia Research University Network (MRUN). It is part of the research program ‘A Big Data Analytics Platform for Optimizing Oil Palm Yield Via Breeding by Design (Grant No: 203.PKOMP.6770007)’ in which a specific project is implemented, ‘Geoinformatics Data for Palm Oil Yield Prediction Using Machine Learning (Vote No: 6300268-10801). FGV R&D Sdn. Bhd. is also acknowledged for providing their expertise and assistance in this research.

6. Conflict of Interests

The authors claim there are no conflicts of interest.

7. References

- [1] Danylo O, Pirker J, Lemoine G, Ceccherini G, See L, McCallum I, et al. A map of the extent and year of detection of oil palm plantations in Indonesia, Malaysia and Thailand. *Sci Data*. 2021;8(1):1–8.
- [2] Chong KL, Kanniah KD, Pohl C, Tan KP. A review of remote sensing applications for oil palm studies. *Geo Spat Inf Sci*. 2017;20(2):184–200.
- [3] Xu K, Qian J, Hu Z, Duan Z, Chen C, Liu J, et al. A New Machine Learning Approach in Detecting the Oil Palm Plantations Using Remote Sensing Data. *Remote Sens*. 2021;13(2):236.

- [4] Atzberger C. Advances in Remote Sensing of Agriculture: Context Description, Existing Operational Monitoring Systems and Major Information Needs. *Remote Sens.* 2013;5(2):949–981.
- [5] Rhyma Purnamasayangsukasih P, Norizah K, Ismail AAM, Shamsudin I. A review of uses of satellite imagery in monitoring mangrove forests. *IOP Conf Ser: Earth Environ Sci.* 2016;37:012034.
- [6] Chang Y, Yan L, Wu T, Zhong S. Remote Sensing Image Stripe Noise Removal: From Image Decomposition Perspective. *IEEE Trans. Geosci. Remote Sens.* 2016;54(12):7018–7031.
- [7] Boiarskii B. Comparison of NDVI and NDRE Indices to Detect Differences in Vegetation and Chlorophyll Content. *JMCMS [Internet].* 2019 [cited 2022 Dec 4];spl1(4). Available from: http://www.journalimcms.org/special_issue/comparison-of-ndvi-and-ndre-indices-to-detect-differences-in-vegetation-and-chlorophyll-content/
- [8] Xue J, Su B. Significant Remote Sensing Vegetation Indices: A Review of Developments and Applications. *J. Sens.* 2017;2017:1–17.
- [9] Mutanga O, Skidmore AK. Narrow band vegetation indices overcome the saturation problem in biomass estimation. *Int. J. Remote Sens.* 2004;25(19):3999–4014.
- [10] Alam AF, Er AC, Begum H. Malaysian oil palm industry: Prospect and problem. *J Food Agric Environ.* 2015;13(2):143–148.
- [11] Darmawan S, Takeuchi W, Haryati A, Najib A M R, Na’aim M. An investigation of age and yield of fresh fruit bunches of oil palm based on ALOS PALSAR 2. *IOP Conf Ser: Earth Environ Sci.* 2016;37:012037.
- [12] Tridawati A, Darmawan S, Armijon. Estimation the oil palm age based on optical remote sensing image in Landak Regency, West Kalimantan Indonesia. *IOP Conf Ser: Earth Environ Sci.* 2018;169:012063.
- [13] Fitrianto AC, Darmawan A, Tokimatsu K, Sufwandika M. Estimating the age of oil palm trees using remote sensing technique. *IOP Conf Ser: Earth Environ Sci.* 2018;148:012020.
- [14] Phiri D, Simwanda M, Salekin S, Nyirenda V, Murayama Y, Ranagalage M. Sentinel-2 Data for Land Cover/Use Mapping: A Review. *Remote Sens.* 2020;12(14):2291.
- [15] Giovos R, Tassopoulos D, Kalivas D, Lougkos N, Priovolou A. Remote Sensing Vegetation Indices in Viticulture: A Critical Review. *Agric.* 2021 May 18;11(5):457.
- [16] Rouse JW, Haas RH, Scheel JA, Deering DW. Monitoring vegetation systems in the great plains with ERTS. In Washington, USA: National Aeronautics and Space Administration; 1974. p. 309–318.
- [17] Fitzgerald GJ, Rodriguez D, Christensen LK, Belford R, Sadras VO, Clarke TR. Spectral and thermal sensing for nitrogen and water status in rainfed and irrigated wheat environments. *Precis. Agric.* 2006;7(4):233–248.
- [18] Huete AR. A soil-adjusted vegetation index (SAVI). *Remote Sens Environ.* 1988;25(3):295–309.
- [19] Gitelson AA, Gritz Y, Merzlyak MN. Relationships between leaf chlorophyll content and spectral reflectance and algorithms for non-destructive chlorophyll assessment in higher plant leaves. *J Plant Physiol.* 2003;160(3):271–282.
- [20] Ostertagová E. Modelling using Polynomial Regression. *Procedia Eng.* 2012;48:500–506.
- [21] Ng SF, Chew YM, Chng PE, Ng KS. An Insight of Linear Regression Analysis. *Sci Res J.* 2018;15(2):1–6.
- [22] Ren H, Zhou G, Zhang F. Using negative soil adjustment factor in soil-adjusted vegetation index (SAVI) for aboveground living biomass estimation in arid grasslands. *Remote Sens Environ.* 2018;209:439–445.
- [23] Yuhao A, Che’Ya NN, Roslin NA, Ismail MR. Rice Chlorophyll Content Monitoring using Vegetation Indices from Multispectral Aerial Imagery. *Pertanika J Sci & Technol.* 2020;28(3):779–795.
- [24] Vallentin C, Harfenmeister K, Itzerott S, Kleinschmit B, Conrad C, Spengler D. Suitability of satellite remote sensing data for yield estimation in northeast Germany. *Precis Agric.* 2022;23(1):52–82.
- [25] Frampton WJ, Dash J, Watmough G, Milton EJ. Evaluating the capabilities of Sentinel-2 for quantitative estimation of biophysical variables in vegetation. *ISPRS J Photogramm Remote Sens.* 2013;82:83–92.
- [26] Imran HA, Gianelle D, Rocchini D, Dalponte M, Martín MP, Sakowska K, et al. VIS-NIR, Red-Edge and NIR-Shoulder Based Normalized Vegetation Indices Response to Co-Varying Leaf and Canopy Structural Traits in Heterogeneous Grasslands. *Remote Sens.* 2020;12(14):2254.